

Magnetic vacancies, ordering, and properties of bismuth-substituted rare-earth ferrite garnets

Yu. P. Vorobyov,* V. G. Bamburov, A. S. Vinogradova-Zhabrova, and N. I. Lobachevskaya

*Institute of Solid State Chemistry, Ural Branch of the Russian Academy of Sciences,
91 Pervomaiskaya, 620219 Ekaterinburg, Russian Federation.
Fax: +7 (343 2) 74 4495. E-mail: korjakin@ihim.uran.ru*

Thermodynamic analysis of the garnet formation processes and crystal chemical simulation of the filling of a garnet crystal lattice with cations were used to identify the types of defects and to estimate their numbers and contributions to the magnetic properties of bismuth-substituted rare-earth scandium-containing ferrogarnets. The effective magnetic moments of the garnets were calculated with allowance for the HS- and LS-states of paramagnetic ions. A classification of crystal defects was proposed. Principles and postulates suitable for any multisublattice and multicomponent crystals were formulated.

Key words: bismuth rare-earth ferrite garnets, defects, thermodynamics, magnetism.

Rare-earth ferrite garnets $R_3Fe_5O_{12}$ (RFG) are widely used as elements of magnetic-optical devices, in which information recording, read-out, and storage are accomplished using single-crystal films with cylindrical magnetic domains.¹

Bismuth-substituted RFG are more promising materials for magnetic optics than basic RFG. At present, the garnet $Bi_3Fe_5O_{12}$ (BIG) is attracting enhanced attention; this material has been synthesized as a film but has not been obtained as bulk ceramics. Independent estimation of the unit cell dimensions for BIG and the valence and magnetic states of the cations is a challenge for crystallography; so are the related problems of isomorphous substitution in BIG, RFG, or solid solutions based on them. In this work, we are attempting to solve this problem.

The basic principles and postulates

The crystals of lanthanide iron oxides $\{R_3\}_{VI}[Fe^{3+}_2]_{VI}(Fe^{3+}_3)_{IV}O_{12}$ belong to the space group $Ia\bar{3}d$ (O_h^{10}), corresponding to a garnet structure with unit cell dimensions of 1.26–1.22 nm and the Neel temperature $T_N = 587$ –548 K or the compensation temperature T_{com} ranging from 5 K (Yb) to 286 K (Gd) and 226 K (Dy).¹ All these compounds are ferrimagnetics. In order to control T_{com} and to match the dimensions of the crystal lattices of the substrate (a_s) to the crystal lattice dimensions of an epitaxially grown RFG-based garnet film (a_f), the latter are doped by double-, triple-, and higher-charged cations. The problems of the epitaxial growth of garnets on various substrates and isomorphous substitution in oxide garnets by various cations into positions 24c, 16a, and 24d of oxide garnets

have been discussed comprehensively and solved in previous publications.^{2–4} It is known¹ that minor replacements of $[Fe^{3+}]_{VI}$ in films by nonmagnetic ions, Ga^{3+} , Al^{3+} , and Sc^{3+} , increase the total magnetization (M) of the garnet, whereas similar substitution in the tetrapositions decreases this value. Moreover, pre-arranged introduction of "magnetic holes," *i.e.*, nonmagnetic ions, into the garnet unit cell markedly changes the strongest exchange interactions, J_{ad} , J_{aa} , and J_{dd} . These changes lead to a decrease or increase in T_C , T_N , and T_{com} and affect the constant of uniaxial growth anisotropy, the coercive force H_C , and the mobility of domains; they influence the Faraday and Kerr effects in the films, *etc.* Magnetic holes in polycrystalline RFG decrease their symmetry and change substantially the unit cell dimensions and magnetic ordering of the garnet. The latter normally decreases not only due to the dilution of magnetic ions by nonmagnetic ions but often also due to a change in the magnetic state of these cations. It follows from Table 1 that transition of the Fe^{2+} and Fe^{3+} ions from the high-spin (HS: $3d^5 \uparrow\uparrow\uparrow\uparrow$) into the low-spin (LS: $3d^5 \uparrow\downarrow\uparrow\downarrow$) state alters substantially their size and magnetic characteristics and results apparently in pronounced changes in the a and M values of the garnet crystal without changing its chemical composition. Hence, the physicochemical problem of determination of the valence states of the ions forming the garnet structure supplemented by a crystallographic problem, *i.e.*, determination of the location and the number of cations in c-, a-, and d sites, becomes complicated by the physical problem of identification of the HS and LS states of magnetic ions. In order to solve this experimental problem, which cannot be solved by X-ray dif-

Table 1. Effective Shannon⁵ ionic radii (r_i /nm) and magnetic moments μ_i (μ_B) of the Fe^{2+} and Fe^{3+} cations located in positions 16a and 24d and occurring in the HS or LS states

State	Fe^{3+}				$[\text{Fe}^{2+}]_{\text{VI}}$	
	octahedral sites		tetrahedral sites		r_i	μ_i
	r_i	μ_i	r_i	μ_i		
HS	0.0645	5	0.049	5	0.078	4
LS	0.0550	1	0.040	1	0.061	0

fraction or magnetometry, we shall use a complex approach proposed⁶ for oxide garnets. This approach includes the following steps.

1. Thermodynamic analysis of the stability of the initial compounds during high-temperature garnet formation and the use of the analysis results to elucidate the nature of technological, structural, and other defects. The types of possible defects are shown in Fig. 1.

2. Crystal-chemical simulation, *i.e.*, determination of the model for the cation distribution over tetra-, octa-, and dodecahedral positions of the garnet, accompanied by estimation of their valence and magnetic states with allowance for the most probable defects.

3. Calculation of the unit cell parameter a_{calc} of the "model" garnet and comparison of the result with the experimental a_{exp} value.

Let us apply this approach to the solid solutions $\text{Dy}_{3-x}\text{Bi}_x\text{Fe}_{5-y}\text{Sc}_y\text{Ga}_z\text{O}_{12}$, synthesized previously.⁷ The samples were prepared from chemically pure Bi_2O_3 , Fe_2O_3 , Ga_2O_3 , Dy_2O_3 , and Sc_2O_3 using ceramic technology. The temperature of the onset of the solid-state

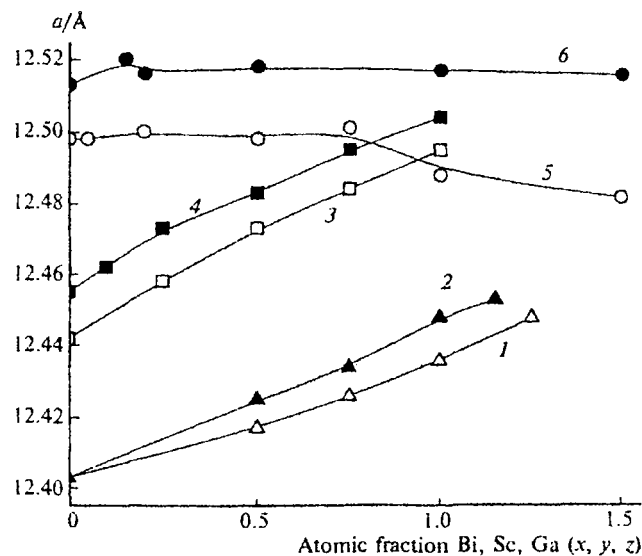


Fig. 1. Change of the lattice parameter as a function of the atomic fraction of (Sc, Bi, Ga) in lanthanide ferrogarnets (1) $\text{Dy}_3\text{Sc}_y\text{Fe}_{5-y}\text{O}_{12}$; (2) $\text{Dy}_{3-x}\text{Bi}_x\text{Fe}_5\text{O}_{12}$; (3) $\text{Dy}_2\text{Bi}_2\text{Sc}_y\text{Fe}_{5-y}\text{O}_{12}$; (4) $\text{Dy}_{1.5}\text{Bi}_{1.5}\text{Sc}_y\text{Fe}_{5-y}\text{O}_{12}$; (5) $\text{Dy}_2\text{BiSc}_{0.75}\text{Ga}_z\text{Fe}_{5-z}\text{O}_{12}$; (6) $\text{Dy}_{1.5}\text{Bi}_{1.5}\text{Sc}_{0.75}\text{Ga}_z\text{Fe}_{5-z}\text{O}_{12}$.

synthesis in air in the initial mechanically homogenized mixtures was 600 °C; after each (of three) trituration of the mixtures, the temperature was raised by 200 °C. The products, which were single-phase materials according to X-ray diffraction data, were powdered down to a particle size of no more than 20 μm , pressed at $p = 1100 \text{ kg cm}^{-2}$, and subjected to homogenizing annealing at 1273 K for 25 h in order to obtain dense ceramics. The concentration dependences of $a(x)$, $a(y)$, and $a(z)$ are shown in Fig. 2.

Thermodynamic analysis⁸ of the equilibrium oxygen pressure p_{O_2} (10^5 Pa) for the dissociation of the initial oxides M_2O_3

	Bi_2O_3	Fe_2O_3	Ga_2O_3	Gd_2O_3	Dy_2O_3	Sc_2O_3
$\log p_{\text{O}_2}$	-4.13	-5.35	-10.37	-40.12	-41.11	-42.04

indicates that all of the oxides are stable at the temperature of the final annealing and, hence, all the cations in the resulting garnets occur in the trivalent state; the anionic and three cationic sublattices are complete and the cation distribution over the c, a, and d sites apparently approaches the equilibrium distribution after 25 h of annealing.

The crystal chemical model of arrangement of the cations over nonequivalent crystallographic positions in the garnet structure implies that large ions mostly occur at the largest oxygen interstices. For instance the high-spin $[\text{Fe}^{3+}]_{\text{VI}}$ ions ($r = 0.0645 \text{ nm}$) preferably occupy the octahedral 16a positions compared to the $[\text{Ga}^{3+}]_{\text{VI}}$ ions

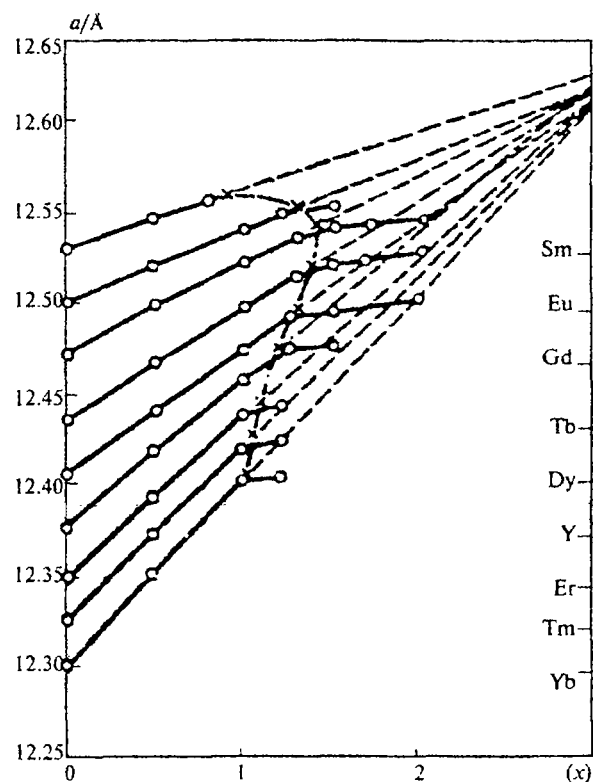


Fig. 2. Dependence of the unit cell parameter of $\text{R}_{3-x}\text{Bi}_x\text{Fe}_5\text{O}_{12}$ on the content of Bi.¹⁴

($r = 0.062$ nm), whereas the low-spin $[\text{Fe}^{3+}]_{\text{VI}}$ ions ($r = 0.055$ nm) let the $[\text{Ga}^{3+}]_{\text{VI}}$ cations occupy these positions. This statement follows from the thermodynamic equilibrium principle, viz., the energy of the system tends to the minimum (for a specified composition, p , p_{O_2} , and T). Apparently, for complex tetrasublattice structures such as garnet, exceptions to this postulate are possible. Thus it is known⁹ that the preference energies E_{ij} for cations to occupy tetra- and octahedral positions in the spinel structure, found by quantum-chemical calculations, show deviations from this principle. Since no calculations of E_{ij} of this type have been carried out for garnets, we shall keep to this principle in our calculations.

The second postulate suggests that the presence of two or more magnetic sublattices in garnets ensures the highest-spin states for the cations that form these crystallographically nonequivalent positions. In the case where magnetic ions occupy only one position (24c, 16a, or 24d), they exist preferably in a low-spin configuration. The validity of this postulate is supported by calculations and studies¹⁰ of the transmission optical spectra of $\text{Y}_3\text{Al}_5\text{O}_{12}$ (Co, Cr), which provided grounds for the conclusion that Co^{2+} ions occupy octahedral positions with a radius of 0.065 nm, corresponding to the low-spin state $[\text{Co}^{2+}]_{\text{VI}}$.⁵

To calculate the crystal lattice parameter of garnet solid solutions, we shall use the most perfect semiempirical formula¹¹

$$a_{\text{calc}} = 10.092217 + 0.841118r_{\text{VIII}} + 0.734598r_{\text{VI}} - 2.507813r_{\text{IV}} + 3.133970r_{\text{VIII}} \cdot r_{\text{IV}} + 1.946901r_{\text{IV}} \cdot r_{\text{IV}} \quad (1)$$

where r_{VIII} , r_{VI} , and r_{IV} are the weight average effective ionic radii⁵ of cations at 24c, 16a, and 24d sites.

The garnets $\text{R}_{3-x}\text{Bi}_x\text{Fe}_5\text{O}_{12}$

Rare-earth garnets $\text{R}_3\text{Fe}_5\text{O}_{12}$ (where R is a lanthanide) were synthesized in 1956,¹² whereas bismuth-containing ferrogarnet was first obtained in 1988 as an epitaxially grown film on the $\text{Gd}_3(\text{ScGa})_5\text{O}_{12}$

substrate ($a_s = 1.2560$ nm) with a unit cell size of 1.2621 nm.¹³

Abnormally high Faraday rotation F on polycrystals and epitaxial films (LPE) of $\text{R}_{3-x}\text{Bi}_x\text{Fe}_5\text{O}_{12}$ (R = Sm–Yb) was first observed in a previous publication¹⁴; this gave impetus to the synthesis and study of numerous Bi-containing garnet compositions. The anomaly of F was interpreted¹⁴ as being due to the high degree of covalence and the high electronegativity of the $\{\text{Bi}^{3+}\}$ cation.

Figure 3 presents the curve for the parameter $a(x)$ for $\text{R}_{3-x}\text{Bi}_x\text{Fe}_5\text{O}_{12}$.¹⁴ It can be seen that the maximum "solubility" of Bi^{3+} in $\text{R}_3\text{Fe}_5\text{O}_{12}$ is a nonlinear function of the ordinal number of the lanthanide n or the number of 4f electrons in the R^{3+} ion. This nonlinearity is due to the change of the ionic radius of $\{\text{Bi}^{3+}\}_{\text{VIII}}$ following isomorphous replacement of the $\{\text{R}^{3+}\}_{\text{VIII}}$ cations.¹⁴ This assumption is at variance with numerous types of systematization, crystal chemical models, and conclusions drawn based on the r_{eff} values; however, there are no grounds for refuting it unless X-ray diffraction or neutron diffraction studies are performed.

Now we estimate the crystal lattice parameters for these garnets at $x = 0.5$ and 1.0 using Eq. (1). It can be seen from Table 2 that for almost all of the indicated garnets, $a_{\text{exp}} > a_{\text{I}}$. This is also true for $\text{R}_3\text{Fe}_5\text{O}_{12}$. Previously, this finding for $\text{Y}_3\text{Fe}_5\text{O}_{12}$ has been interpreted⁶ and thermodynamically substantiated¹⁵ by assuming the formation of $[\text{Fe}^{2+}]_{\text{VI}}$ because of partial dissociation of the ferrite. Having calculated the a_{II} value for the $\text{II} \cdot \{\text{R}_{3-x}\text{Bi}_x\}[\text{Fe}^{2+}\text{Fe}^{3+}](\text{Fe}^{3+}_3)\text{O}_{11.5}$ component using Eq. (1), one can find c_{Fe} , viz., the number of $[\text{Fe}^{2+}]_{\text{VI}}$ ions and the deviation from stoichiometry, $\delta = c/2$.

Analysis of the data presented in Table 2 shows that all of the garnets prepared¹⁴ are defective and nonstoichiometric. The most abundant defects are $[\text{Fe}^{2+}]_{\text{VI}}$ cations and anionic vacancies. The number of these defects does not change with an increase in x to within the error of calculations or measurements of a_{exp} (except for the dysprosium garnet). The invariability of $c_{\text{Fe}^{2+}}$ (at a given R) implies that bismuth ions are chemically inert, and the exception observed for $\text{Dy}_{3-x}\text{Bi}_x\text{Fe}_5\text{O}_{12}$ is apparently due to the magnetic influence of Dy^{3+} , which

Table 2. Unit cell parameters (a/nm) for the $\text{R}_{3-x}\text{Bi}_x\text{Fe}_5\text{O}_{12}$ films¹³ and the components $\{\text{R}^{3+}_{3-x}\text{Bi}^{3+}_x\}[\text{Fe}^{3+}_2](\text{Fe}^{3+}_3)\text{O}_{12}$ (I) and $\{\text{R}^{3+}_{3-x}\text{Bi}^{3+}_x\}[\text{Fe}^{2+}\text{Fe}^{3+}](\text{Fe}^{3+}_3)\text{O}_{11.5}$ (II), calculated from Eq. (1), and $c_{\text{Fe}^{2+}}$, the number of $[\text{Fe}^{2+}]$ (formula units) in garnets

R	$x = 0.5$				$x = 1.0$			
	a_{exp}	a_{I}	a_{II}	$c_{\text{Fe}^{2+}}$	a_{exp}	a_{I}	a_{II}	$c_{\text{Fe}^{2+}}$
Sm	1.2548	1.2548117	—	0	1.2561	1.255904	1.267302	0.02
Eu	1.2518	1.2511506	1.2625485	0.06	1.2538	1.2463969	1.2577498	0.09
Gd	1.2497	1.2491698	1.2605677	0.05	1.2522	1.2511506	1.2625485	0.09
Tb	1.2468	1.2452086	1.2566065	0.14	1.2494	1.2448125	1.2562104	0.12
Dy	1.2428	1.2432279	—	0	1.2472	1.2463969	1.2577944	0.07
Y	1.2419	1.2402569	1.2516548	0.14	1.2456	1.2440202	1.2554181	0.14
Er	1.2390	1.2372860	1.2486839	0.15	1.2439	1.2416435	1.2530414	0.20
Tm	1.2372	1.2353054	1.2467033	0.17	1.2420	1.2400590	1.2514569	0.17
Yb	1.2353	1.2333248	1.2447227	0.17	1.2402	1.2384744	1.2498723	0.15

possesses the largest intrinsic magnetic moment, equal to $9 \mu_B$.⁹ To estimate this influence qualitatively, we studied single-phase solid solutions $Dy_{3-x}Bi_xFe_5O_{12}$, synthesized previously.⁷ Table 3 presents the a_{exp} values and a_{calc} values found from Eq. (1). It can be seen from the comparison that $a_{exp} > a_{calc}$ and that the difference $\Delta = a_{exp} - a_{calc}$ increases with increase in the number of $\{Bi^{3+}\}_{VIII}$. According to the results of thermodynamic analysis, the ions present in this system do not change their valence states. Therefore, it can be assumed that the deviation of the unit cell dimensions from the values found from Eq. (1) is due to a change in the magnetic state of either only the iron cations (model I) or all the magnetic ions (model II).

Analysis of the calculation results indicates (see Table 3) that model II ensures a higher magnetic order. This can be seen especially clearly for $x = 1.15$. In this case, the limiting isomorphous replacement in the dodecahedra (at given p , p_{O_2} , and T) and the maximum magnetic ordering are attained simultaneously.

It was of interest to carry out these calculations for a system containing a diamagnetic lanthanide ion, for example, for $Y_{3-x}Bi_xFe_5O_{12}$.^{13,16-19} The Bi^{3+} ion is also diamagnetic. Nevertheless, the replacement of $\{Y^{3+}\}$ by $\{Bi^{3+}\}$ linearly changes the Curie (Néel) temperature by +33 K per Bi in the formula unit. NMR studies of a bismuth-substituted iron-yttrium garnet²⁰ showed that Bi^{3+} has an internal field with H_{in} equal to 60 kOe, which points to the existence of a local intrinsic magnetic moment of this ion. This unusual fact necessitates not only additional experimental and theoretical studies but attests to the occurrence of complex interatomic interactions in the crystal following the isomorphous replacement of magnetic ions in the lattice by diamagnetic ions. No anomalous features were found in the temperature dependence (15–600 K) of F , i.e., the Faraday rotation for BIG¹⁷; therefore it was concluded²¹ that the bismuth ferrite garnet, like $R_3Fe_5O_{12}$, is a collinear ferrimagnetic.^{1,9,12} This indirectly implies that the statement²⁹ about the presence of H_{in} at the $\{Bi^{3+}\}_{VIII}$ ions in BIG is incorrect and, hence, the Néel model can be used to calculate the effective magnetic moments of garnet solid solutions $R_{3-x}Bi_xFe_5O_{12}$ (R is a lanthanide

or Y). An example of this calculation of μ_{exp} for $Dy_{3-x}Bi_xFe_5O_{12}$ is presented in Table 3, which shows a clear-cut decrease in μ_{exp} following an increase in x .

The $Y_{3-x}Bi_xFe_5O_{12}$ films, like BIG, were synthesized¹⁷ by spraying a target (garnet + excess Bi_2O_3) on a garnet substrate with a high-energy (1.5–5 keV) ion beam in a high vacuum ($p = 1.07 \cdot 10^{-3}$ Pa). According to the data reported previously,¹⁷ the crystal lattice parameter for the above-mentioned solid solutions changes linearly

$$a_{exp} = 1.23756 + 0.0828x \text{ (nm)}. \quad (2)$$

It is known⁸ that Bi_2O_3 is the most stable of bismuth oxides and that this oxide vaporizes congruently. Redox disproportionation of bismuth(+3) ions is unfavorable for thermodynamic reasons. $[Fe^{2+}]_{VI}$ ions are more likely to appear due to partial dissociation of Fe_2O_3 in the garnet during its ion-plasma jet spraying and heating *in vacuo*. Comparison of the crystal lattice parameters calculated using Eq. (1) with the experimental values calculated using Eq. (2) demonstrates (Table 4) that $a_{exp} > a_{calc}$. This indirectly confirms the thermodynamic conclusions, because a_F , the unit cell dimension of an epitaxially grown film, depends not only on the composition and spraying conditions (p , p_{O_2} , T , τ) but also on the a_S value of the substrate.

Table 4 contains (variant I) the experimental values for the unit cell parameter for BIG films as functions of the dimension a_S of the garnet substrate. Analysis of the presented characteristics shows that the larger a_S , the closer the dimension a_F of the epitaxially grown garnet film (for $SmScGaG$, they are equal) and the smaller the value $\Delta = a_F - a_S$. The precise a_{exp} value for single-crystal or polycrystalline ceramic (three-dimensional) BIG is unknown. The bismuth ferrogarnet is a thermodynamically metastable phase¹⁶⁻¹⁹; therefore, a three-dimensional BIG crystal has not been synthesized yet. Moreover, the a_F value depends on the method of synthesis, the film thickness, and the determining external parameters p , T , and p_{O_2} . The latter follows from Table 4 (variant II); a slight difference in the rate of oxygen supply to the system, v_{O_2} , all other factors being the same, substantially influences the unit cell parameter a_F . In other words, the more oxygen gets into the system, the smaller the number of $[Fe^{2+}]_{VI}$ defects and the closer the a_{exp} value to the equilibrium value for given (p , T) conditions. This finding confirms the validity of both our thermodynamic analysis and our choice of the predominant type of defects in the BIG films synthesized by ion-plasma jet spraying of a garnet target *in vacuo*.

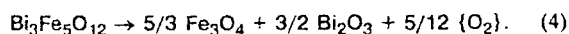
The difficulties in interpretation of the a_{exp} values for Bi-substituted garnets are well known. Thus the Shannon⁵ ionic radius of $\{Bi^{3+}\}_{VIII}$, equal to 0.111 nm, was arbitrarily increased²² to 0.1132 nm, which allowed the calculated a_{calc} values for these garnets to be matched to experimental results, a_{exp} . Let us estimate a_{calc} for $Bi_3Fe_5O_{12}$ using these $r_{Bi^{3+}}$ values and Eqs. (1) and (3):

Table 3. Experimental ($a_{exp} \pm 0.003$) and calculated (a_{calc})¹ crystal lattice parameters for $Dy_{3-x}Bi_xFe_5O_{12}$, the high-spin states of magnetic cations (c) calculated in terms of models I and II, and magnetic moments of saturation (μ_{eff}) in model II

Parameter	x				
	0	0.5	0.75	1.0	1.15
a_{exp}/nm	1.2403	1.2425	1.2434	1.2448	1.2453
a_{calc}^I/nm	1.240059	1.243228	1.244812	1.246397	1.252760
$c_{HS}^I/mole \text{ fr.}$	1.0	0.98	0.96	0.95	0.77
$c_{II}^I/mole \text{ fr.}$	1.0	0.984	0.968	0.964	0.847
$\mu_{eff}^I(\mu_B)$	21.9	17.2	14.8	12.4	10.0

$$a_{\text{calc}} = 7.02954 + 3.31277(r_{\text{VII}}) + \\ + 2.49398(r_{\text{VI}}) + 3.34124(r_{\text{IV}}) - \\ - 0.87758(r_{\text{VII}})(r_{\text{VI}}) - 1.38777(r_{\text{VII}})(r_{\text{IV}}). \quad (3)$$

As follows from analysis of the a_{calc} and a_{exp} values listed in Table 5, all of the experimental values for the crystal lattice parameter for BIG lie in the $a_{\text{III}} < a_{\text{exp}} < a_{\text{I}}$ range. Moreover, a_{IV} coincided with the a_{exp} value for the bismuth ferrigarnet films studied most accurately.¹⁹ In our opinion, $a_{\text{BIG}} = 1.2539 \pm 0.0002$ nm is the most acceptable (and really existing) value for polycrystalline materials (powders or ceramics). This is indicated by the fact (see Table 4, variant II) that neither an increase in the film thickness, $1.45 \leq l \leq 1.90$, nor change in the velocity of the oxygen supply to the setup, nor even the difference in the dimensions of the crystal lattice of the substrate (1.2353 and 1.2627 nm) influence the value $a_{\text{S}} = 1.2538 \pm 0.0001$ nm. The latter characteristic is entirely controlled and determined by the pressure of oxygen (in this particular case, the velocity of the stream or flow rate). It can be assumed that this value is close to the equilibrium $p_{\text{O}_2}(\text{p})$; therefore, an increase in p_{O_2} to atmospheric pressure should not change the BIG composition. However, when the synthesis is carried out in a high vacuum, i.e., at $p_{\text{O}_2} \ll p_{\text{O}_2}(\text{p})$, the bismuth garnet necessarily dissociates, and in the case of long reaction times ($\tau \geq 10$ h), it can decompose according to the following reaction:



The partial dissociation is accompanied by removal of oxygen from the crystal and formation of anionic vacancies and an equivalent number of $[\text{Fe}^{2+}]_{\text{VI}}$. It is the latter species that are responsible, in our opinion, for the large scatter in the a_{exp} values (obtained by different researchers), because each experiment was characterized by a particular set of determining external parameters, p , T , and p_{O_2} , the spraying time, and the size, temperature,

and composition of the substrate, which were different in various studies. Analysis of the crystal structure of polycrystalline thin films of $\text{Bi}_3\text{Fe}_5\text{O}_{12-\delta}$, carried out¹⁹ using symmetrical (SS) and asymmetrical (ASS) X-ray technique showed that conclusions based on these studies for the same samples do not agree with one another and, therefore, they should be treated with caution. In addition, it was found¹⁹ that the films under study are nonstoichiometric, and $\delta = 0.06$ (from the SS data) or 0.27 (from the ASS data). Our calculation using Eq. (1) for $a_{\text{F}} = 1.26473$ nm gave the value $\delta = 0.04$. However, although these values seem to be close, the natures of this oxygen nonstoichiometry, i.e., incompleteness of the anionic sublattice, are absolutely different. It may be due to, among other factors, dissociation of the garnet film *in vacuo* during spraying and formation of $[\text{Fe}^{2+}]_{\text{VI}}$, although the researchers cited claim¹⁹ that bismuth vacancies $\{\text{V}^0_{\text{Bi}}\}$ are formed in dodecahedral sites. Analysis that we carried out previously attests that the formation of $\{\text{V}^0_{\text{Bi}}\}$ is thermodynamically forbidden. In addition, Bi_2O_3 dissociates congruently.⁸ The formation of these large vacancies is energetically unfavorable, unlike the process $[\text{Fe}^{3+}]_{\text{VI}} + [\text{O}_0^{2-}] \rightarrow [\text{Fe}^{2+}]_{\text{VI}} + [\text{O}_0^{1-}]$, whose energy in ferrites (according to Ref. 23) does not exceed 2.5 eV. Finally, the formation of cationic vacancies should decrease the unit cell dimensions, whereas the experiment shows that $a_{\text{exp}} > a_{\text{calc}}$. Therefore, the question of the nature and number of defects in BIG should be solved separately for each sample, taking into account its whole technological prehistory. Measurements of magnetic properties alone also do not answer the question of what is the nature of defects in the garnet studied. Only a complex approach,⁶ analysis of the results obtained by various physical methods or neutron diffraction and spectroscopic (NGR, NMR, ESR, etc.) studies can altogether bring us closer to solution of this complicated physicochemical problem. The difficulties arising during interpretation have been considered tak-

Table 4. Crystal lattice parameters (a_{F}) for $\text{Bi}_3\text{Fe}_5\text{O}_{12}$ films synthesized on different-size garnets (a_{S}) (model I) for various flow rates of O_2 (ν_{O_2}) (model II)

Parameter	Model	Substrate material (a_{S} /nm)				Method (reference)
		YIG (1.2388) ^a	GGG (1.2488) ^a	BiDyIGaG (1.2353) ^a	$\text{Sm}_3(\text{SeGa})_5\text{O}_{12}$ (1.2627) ^a	
l_{F} /nm	I	0.637	0.874	1.017	1.62	(18)
a_{F} /nm		1.2660	1.2653	1.2661	1.2626	(18)
Δ /nm		0.0272	0.0165	0.0308	-0.0001	
ν_{O_2} /cm ³ s ⁻¹	II	0.1	0.2	0.3	0.4	(16)
l_{F} /μm		1.10	1.05	1.45	1.90	RIBS ^b
a_{F} /nm		1.2547	1.2543	1.2537	1.2539	
a_{F} /nm	III	1.2648(1) ^c	1.26469(3) ^d	1.2647(1) ^d		(19)

^a RRFS is reaction radiofrequency technology.

^b RIBS is reaction ion beam spraying.

^c Analysis was carried out using ASS X-ray technique.

^d Using SS X-ray technique.

Table 5. Unit cell parameters ($a_{\text{calc}}/\text{nm}$) of bismuth ferrogarnets calculated from Eqs. (1) and (3)

$r_{\{\text{Bi}^{3+}\}_{\text{VIII}}}/\text{nm}$	Fe ³⁺ spin state	Model	Composition	a_{calc} (1)	a_{calc} (3)	a_{exp}
0.111	HS	I	$\{\text{Bi}_3\}[\text{Fe}^{3+}_2](\text{Fe}^{3+}_3)\text{O}_{12}$	1.25907	1.25694	1.2539—
	LS	II	$\{\text{Bi}_3\}[\text{Fe}^{3+}_2](\text{Fe}^{3+}_3)\text{O}_{12}$	1.21362	1.22630	—1.2547 ¹⁶
	HS	III	$\{\text{Bi}_3\}[\text{Fe}^{2+}\text{Fe}^{3+}](\text{Fe}^{3+}_3)\text{O}_{11.5}$	1.27047	1.26720	1.26610 ¹⁸
0.1132	HS	IV	$\{\text{Bi}_3\}[\text{Fe}^{3+}_2](\text{Fe}^{3+}_3)\text{O}_{12}$	1.26431	1.26149	1.26473 ¹⁹
	HS	V	$\{\text{Bi}_3\}[\text{Fe}^{2+}\text{Fe}^{3+}](\text{Fe}^{3+}_3)\text{O}_{11.5}$	1.27570	1.27102	

ing a NGR study²¹ of the magnetic properties of BIG films as an example, because the detection²⁰ of an intrinsic magnetic field, equal to 60 kOe, at $\{\text{Bi}^{3+}_{\text{VIII}}\}$ implies that this ion is magnetically active and all electromagnetic characteristics of RFG can be substantially changed by doping with bismuth. Analysis of the NGR spectra (Table 6) shows that all the parameters change almost linearly as x increases from 0 to 3. This fact contradicts the occurrence of a large H_{in} at $\{\text{Bi}^{3+}_{\text{VIII}}\}$ ions. The $\text{Fe}^{2+}_{\text{VI}}$ numbers in films, calculated from Eq. (1), indicate that, first, in line with our crystal chemical model, iron(2+) ions occupy positions 16a; and second, it is these ions that cause the most significant magnetic perturbations in the crystal: for the maximum $c = 0.52$ ($x = 2.5$), the quadrupole splitting of Fe in octahedral sites corresponds to the minimum, $EQQ = 0.0025 \text{ mm s}^{-1}$. This fact can be regarded as direct experimental evidence of the correctness of not only Eq. (1) but also the whole complex approach to estimation of the nature and calculation of the number of defects in oxide garnets. The maximum nonstoichiometry value, found by the asymmetrical X-ray method²¹ and equal to 0.27, corresponds to the value of 0.26 ± 0.01 found in our calculations.

According to the model,²⁴ the overall magnetic moment of saturation of BIG is the algebraic sum of the contributions of the moments of three sublattices

$$\mu_{\text{eff}} = (\mu_{\text{IV}} - 0.5\mu_{\text{B}}) - \mu_{\text{VI}} - (\mu_{\text{VIII}} + 0.2\mu_{\text{B}}). \quad (5)$$

It can be seen from Eq. (5) that, within the framework of this model, the bismuth dodecahedral sublattice contributes to the magnetic moment, $\mu = 0.2\mu_{\text{B}}$, due to either charge transfer from $\{\text{Bi}^{3+}_{\text{VIII}}\}$ to $[\text{Fe}^{3+}_{\text{IV}}]$ or the formation of the hybrid complex $\{\text{Bi}-\text{O}-\text{Fe}_{\text{VI}}\}$. In our

opinion, it is more acceptable to interpret the presence of μ_{VIII} , a magnetic moment in the dodecahedral sublattice of the BIG films studied previously,²⁴ by assuming that some of the Fe^{2+} cations fall into the dodecahedra when they pass from the target to the film. If we take $\mu(\text{Fe}^{2+}) = 4\mu_{\text{B}}$, the number of these ions in the dodecahedra $c \approx 0.2/4 = 0.05$. This value is quite admissible and realistic for a high-frequency spraying procedure.

The garnets $\text{Dy}_{3-x}\text{Bi}_x\text{Fe}_{5-y-z}\text{Sc}_y\text{Ga}_z\text{O}_{12}$

The foregoing makes it possible to apply the complex thermodynamic and crystal chemical approach to a more complicated garnet system, $\text{Dy}_{3-x}\text{Bi}_x\text{Fe}_{5-y-z}\text{Sc}_y\text{Ga}_z\text{O}_{12}$, synthesized previously.⁷ Table 7 presents the a_{exp} values and the crystal lattice parameters calculated for $\{\text{Dy}_3\}[\text{Fe}_{2-y}\text{Sc}_y](\text{Fe}_3)\text{O}_{12}$ in terms of model II using Eq. (1) with allowance for only the high-spin ($a^{\text{II}}_{\text{HS}}$) or only the low-spin ($a^{\text{II}}_{\text{LS}}$) state. It can be seen from comparison that $a_{\text{LS}} < a_{\text{exp}} < a_{\text{HS}}$. The effective magnetic moments μ_{eff} calculated in terms of the collinear Neel model diminish with an increase in y , due not only to a decrease in $[\text{Fe}^{3+}]$ but also to the appearance of low-spin states of the $\{\text{Dy}^{3+}_{\text{VIII}}\}$, $\{\text{Fe}^{3+}_{\text{VI}}\}$, and $[\text{Fe}^{3+}_{\text{IV}}]$ ions.

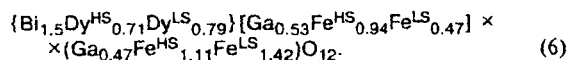
The initial composition of the ceramic target used²⁵ to synthesize the Bi—Dy—Ga—I—G films by laser pulse spraying was $\text{Bi}_{1.5}\text{Dy}_{1.5}\text{Fe}_4\text{GaO}_{12}$ ($a_{\text{exp}} = 1.2555 \pm 0.0005 \text{ nm}$). The researchers cited²⁵ did not study the film composition but it presumably did not coincide with the composition of the target. If we assume that the distribution of the cations and valences in a garnet target correspond to the formula $\{\text{Bi}^{3+}_{1.5}\text{Dy}^{3+}_{1.5}\}[\text{Fe}^{3+}_2](\text{Ga}^{3+}\text{Fe}^{3+}_2)\text{O}_{12}(\text{I})$, then it fol-

Table 6. Physical parameters (H_{in} , IS , EQQ) of the NGR spectrum,²¹ unit cell parameters (a_{exp}), number of $[\text{Fe}^{2+}_{\text{VI}}]$ ions (c), and saturation magnetic moments (μ_{eff}) for the $\text{Y}_{3-x}\text{Bi}_x\text{Fe}_5\text{O}_{12-\delta}$ garnet films ($\delta = c/2$)

Composition, x	a_{exp}/nm	$4\pi M_{\text{S}}/\text{G}$	H_{in}/kOe		$IS/\text{mm s}^{-1}$		$EQQ/\text{mm s}^{-1}$		$c_{[\text{Fe}^{2+}_{\text{VI}}]}$ (form. unit)	$\mu_{\text{eff}} (\mu_{\text{B}})$
			16a	24d	16a	24d	16a	24d		
0	1.2376	1740	486	391	0.3771	0.1561	0.0237	0.0249	0.09	4.91
0.5	1.2419	—	—	—	—	—	—	—	0.14	4.86
2.0	1.2554	—	—	—	—	—	—	—	0.23	4.77
2.5	1.2612	—	489	417.5	0.3960	0.2116	0.0025	0.0166	0.52	4.48
3.0	1.2628	1500	491	421	0.4024	0.2032	0.0295	0.0299	0.33	4.67

Note. $4\pi M_{\text{S}}$ is the saturation magnetization, H_{in} is the internal field, IS is the chemical shift, EQQ is the quadrupole splitting.

lows from Eq. (1) that $a_1 = 1.30238$ nm if all the magnetic ions exist in HS states. For the component $\{\text{Bi}^{3+}_{1.5}\text{Dy}^{3+}_{1.5}\}[\text{Ga}^{3+}\text{Fe}^{3+}](\text{Fe}^{3+}_3)\text{O}_{12}(\text{II})$, Eq. (1) gives $a_{\text{II}} = 1.21320$ nm if all the magnetic ions are in LS states. Apparently, the state of the target is intermediate (nearly 1 : 1 = HS : LS) between I and II, namely,



Analysis of Eq. (6) leads to the following conclusions:

(1) introduction of nonmagnetic Ga^{3+} ions in a quantity of 1.0 atom per formula unit into DyIG (see Table 3) causes a more pronounced perturbation of the magnetic subsystem, compared with that for Bi^{3+} . (This was to be expected because Ga^{3+} ions, which occupy positions 16a and 24d in the garnet, affect the strongest exchange interactions; the exchange integrals for $\text{R}_3\text{Fe}_5\text{O}_{12}$ are the following:²⁶ $J_{\text{ad}} \approx -36$ K, $J_{\text{dd}} \approx -15$ K, and $J_{\text{aa}} = -8$ K, whereas $J_{\text{dc}} \approx -4$ K, $J_{\text{ac}} \approx -0.4$ K, and $J_{\text{cc}} \approx -0.1$ K);

(2) model II is more realistic than model I, since it takes into account the magnetic disorder in all three cationic sublattices;

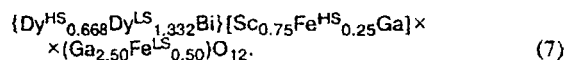
(3) the distribution of Ga^{3+} cations over nonequivalent crystallographic positions a and d (Eq. (5)) does not correspond to statistical distribution and does not reveal any preference to either octahedral or tetrahedral oxygen environment.

An X-ray diffraction study¹⁹ of the distribution of Ga^{3+} ions over the a and d sites in the garnets $\text{Bi}_2\text{DyGa}_{2.5}\text{Fe}_{2.5}\text{O}_{12}$ also did not demonstrate preference of these ions to either of these positions; hence, the earlier conclusions¹⁹ fully coincide with ours. This is one more experimental proof confirming the validity of our approach and the conclusions drawn.

The synthesis of $\text{Dy}_2\text{BiGa}_5\text{O}_{12}$ ($a_{\text{exp}}^* = 1.2295$ nm) and $\text{Dy}_{1.5}\text{Bi}_{1.5}\text{Ga}_5\text{O}_{12}$ ($a_{\text{exp}}^* = 1.2293$ nm) has shown⁷ that the samples are not single-phase materials and have equal a_{exp}^* . This may point to the existence of a limit of the isomorphic replacement of dysprosium by bismuth. This limit can be easily estimated from Eq. (1) with the assumption that the Dy^{3+} ions in $\{\text{Dy}_{3-x}\text{Bi}_x\}[\text{Ga}_2](\text{Ga}_3)\text{O}_{12}$ exist in a low-spin state, (pos-

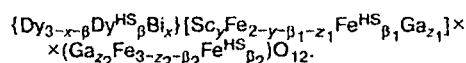
tulate II) and $x = 2.06$. The calculation shows that the limit of solubility has not yet been attained in these samples and their phase inhomogeneity is apparently due to the fact that the solid-state garnet-formation reactions have not come to completion.

Crystal chemical analysis of the previously synthesized⁷ garnet $\text{Dy}_2\text{BiSc}_{0.75}\text{Fe}_{0.75}\text{Ga}_{3.5}\text{O}_{12}$ ($a_{\text{exp}} = 1.2432$ nm), shown to be a single-phase sample by X-ray diffraction analysis, identified the following types of distribution of trivalent cations (long-range order λ) and the following magnetic states (magnetic ordering, c_{HS}):



The presence of magnetic holes (diamagnetic ions) in all three cationic sublattices has a substantial effect on λ and c_{HS} .

Tables 8 and 9 present the results of this type of analysis for solid solutions of the garnets



The β , β_1 , β_2 , z_1 , z_2 , and c_{HS} values were estimated and the effective magnetic moments of saturation μ_{eff} were calculated in terms of the Neel model. It was assumed (in conformity with Ref. 8) that the magnetic moments of Dy^{HS} and Fe^{HS} are 9 and 5 μ_{B} and those of Dy^{LS} and Fe^{LS} are equal to 1 μ_{B} . All these garnets (see Tables 8 and 9) are stoichiometric, according to the data of thermodynamic analysis, and the defects in them are represented by not only magnetic vacancies but also low-spin cations. The calculated μ_{eff} values (μ_{B}) for $\text{Dy}_{3-x}\text{Bi}_x\text{Sc}_y\text{Fe}_{5-y}\text{O}_{12}$ (DBSIG) and $\text{Dy}_{3-x}\text{Bi}_x\text{Sc}_{0.75}\text{Ga}_z\text{Fe}_{4.25-z}\text{O}_{12}$ are presented in Fig. 3: $x_1 = 1$ (curve 1) and $x_2 = 1.5$ (curve 2). As was to be expected, the total magnetic moment of DBSIG smoothly decreases with an increase in $[\text{Sc}^{3+}]$ in octahedral sites, whereas the replacement of magnetic Fe^{3+} cations in DBSIG by diamagnetic Ga^{3+} ions (see Fig. 3) increases this value up to $z \approx 2$ and decreases it at $z > 2$. This can formally be explained by the fact that up to $z < 2$, the substitution occurs in octahedral sites, whereas after $z > 2$, it involves tetrahedral positions. However, our calculations showed that Ga^{3+} ions occupy (as their number in solid solutions increases) both the 16a and 24d sites. The fact that they prefer to occupy the 24d positions is explained by the crystal chemical postulate, because their sizes, $r_{\text{VI}} = 0.062$ and $r_{\text{IV}} = 0.047$ nm, are smaller than the radii of the $[\text{Fe}^{3+}]_{\text{VI}}$ (HS) and $[\text{Fe}^{3+}]_{\text{IV}}$ (HS) ions, respectively (see Table 1).

Analysis of the results obtained (see Tables 8 and 9) also indicates that as the number of diamagnetic ions in garnet crystals increases, the number and proportion of high-spin states of the cations c_{HS} decreases. When the garnet contains one magnetic sublattice, paramagnetic cations are likely to exist predominantly in a low-spin state. This phenomenon is known and has been confirmed experimentally, for example, for LiCoO_2 or

Table 7. Crystal lattice parameters (a_{exp}) for the $\{\text{Dy}_3[\text{Fe}_{2-y}\text{Sc}_y](\text{Fe}_3)\text{O}_{12}$ garnets, calculated numbers (c) of high-spin Fe^{3+} ions (model I) or ($\text{Dy}^{3+} + \text{Fe}^{3+}$) ions (model II), and saturation magnetic moments (μ_{eff})

Parameter	Model	y			
		0.5	0.75	1.0	1.25
a_{exp}/nm		1.2417	1.2426	1.2436	1.2448
$a_{\text{II}}^{\text{HS}}/\text{nm}$		1.2443	1.2464	1.2485	1.2506
$a_{\text{II}}^{\text{LS}}/\text{nm}$		1.1985	1.2022	1.2059	1.2096
$c_{\text{HS}}/\text{mole fr.}$	I	0.91	0.86	0.81	0.76
	II	0.94	0.91	0.88	0.86
$\mu_{\text{eff}} (\mu_{\text{B}})$	II	18.7	17.2	15.7	14.4

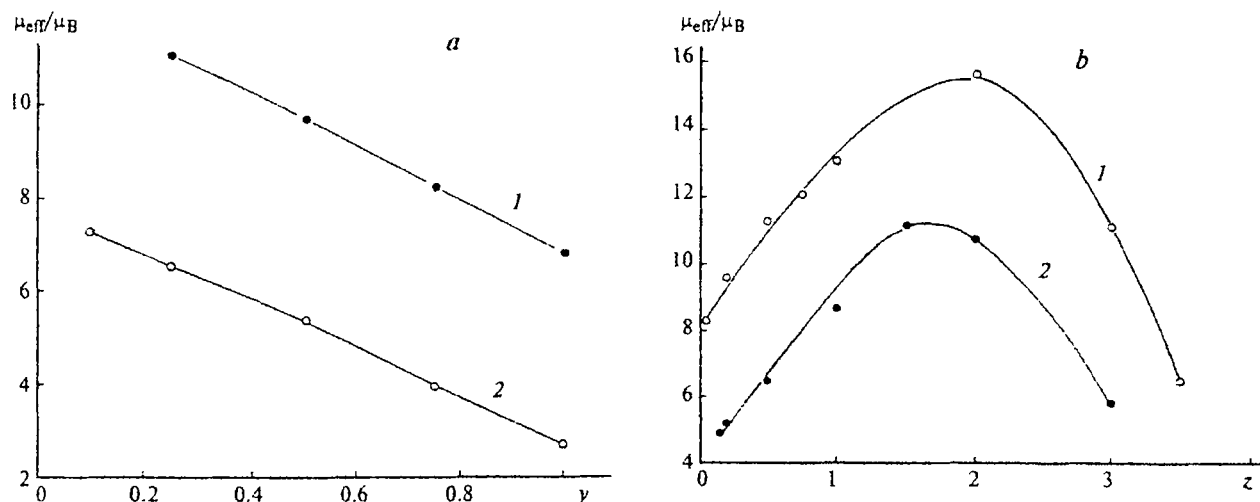


Fig. 3. Concentration plots for the magnetic moments μ_{eff} (μ_B) for $\text{Dy}_{3-x}\text{Bi}_x\text{Sc}_y\text{Fe}_{5-y}\text{O}_{12}$ (a) and $\text{Dy}_{3-x}\text{Bi}_x\text{Sc}_{0.75}\text{Ga}_z\text{Fe}_{4.25-z}\text{O}_{12}$ (b): (1) for $x = 1$; (2) for $x = 1.5$.

LiNiO_2 ,²⁷ in which the Co^{2+} and Ni^{2+} ions are in LS states. The low-spin states of trivalent lanthanide ions $\text{R}^{3+}_{\text{LS}}$ have been considered in a monograph published previously.²⁹

The formation of magnetic holes in any cationic sublattice of the garnet changes the energy of exchange

integrals. This results in a substantial change of the nature of the defects in the garnet structure, caused not only by reorientation of electron spins but apparently also by a change in the spin-orbital moments, and, perhaps, nuclear spins. Relatively high concentrations of different-valence ions and cationic or anionic vacancies favor the formation of complex defects, clusters. The presence of these inhomogeneities strongly affects the electrophysical, magneto-optical, and crystallographic characteristics of single crystal and polycrystalline oxides, films, and ceramics.^{30,31}

The above-considered data concerning isomorphism and behavior of bismuth-substituted compounds $\text{R}_3\text{Fe}_5\text{O}_{12}$ upon introduction of diamagnetic ions (magnetic vacancies) lead to the following conclusions:

The systematization of technological defects in crystals proposed here points to the crucial role of technology in the formation of defect crystals.

Thermodynamic analysis of garnet-formation processes, crystal chemical simulation and the perfect analytical de-

Table 8. Unit cell parameters ($a_{\text{exp}} \pm 0.0003$), magnetic ordering (c_{HS}), and effective saturation magnetic moments μ_{eff} for $\text{Dy}_{3-x}\text{Bi}_x\text{Sc}_y\text{Fe}_{5-y}\text{O}_{12}$ ($x = 1.0/1.5$)

Parameter	y				
	0.1	0.25	0.5	0.75	1.0
a_{exp}/nm	—	1.2458	1.2473	1.2484	1.2495
	1.2462	1.2473	1.2483	1.2495	1.2504
c_{HS}	—	0.936	0.919	0.890	0.859
/mole fr	0.897	0.891	0.888	0.827	0.785
μ_{eff}	—	11.05	9.69	8.26	6.87
(μ_B)	7.27	6.54	5.38	3.97	2.75

Table 9. Experimental values a_{exp} and calculated magnetic ordering parameters (c_{HS}), effective saturation magnetic moments (μ_{eff}), and number of $[\text{Ga}^{3+}]_{\text{VI}}$ in $\text{Dy}_{3-x}\text{Bi}_x\text{Sc}_{0.75}\text{Ga}_z\text{Fe}_{4.25-z}\text{O}_{12}$ ($x = 1.0/1.5$)

Parameter	$z/\text{form. unit}$								
	0.05/0.15	0.20	0.50	0.75	1.0	1.5	2.0	3.0	3.5
a_{exp}/nm	1.2498	1.2500	1.2498	1.2501	1.2488	—	1.2476	1.2468	1.2432
	1.2520	1.2516	1.2518	—	1.2517	1.2516	1.2876	1.2454	—
c_{HS}	0.928	0.936	0.938	0.951	0.923	—	0.912	0.928	0.333
/mole fr.	0.898	0.883	0.899	—	0.874	0.922	0.825	0.702	—
μ_{eff} (μ_B)	8.3	9.6	11.3	12.1	13.1	—	15.7	11.2	6.6
	4.9	5.2	6.5	—	8.7	11.2	10.8	5.9	—
$[\text{Ga}^{3+}]_{\text{VI}}$	0.02	0.01	0.03	0.04	0.08	—	0.11	0.09	1.0
/form. unit	0.01	0.03	0.06	—	0.09	0.10	0.22	0.37	—

pendence $a_{\text{calc}} = f(r)$ make it possible to elucidate the nature of unit cell defects and estimate the number of these defects and their contribution to the physical, including magnetic, properties of multicomponent garnet solid solutions based on $\text{R}_3\text{Fe}_5\text{O}_{12}$ and $\text{Bi}_3\text{Fe}_5\text{O}_{12}$.

Taking BIG as an example, it was shown that the transition from vacuum spraying technology to solid-state synthesis ensures the replacement of defects from $[\text{Fe}^{2+}]_{\text{VI}}$ and V''_{O} to $\text{Fe}^{3+}(\text{LS})$ and $\text{R}^{3+}(\text{LS})$, respectively.

It was found that crystal chemical models I and II are noncontradictory. The conclusions based on these models concerning the cation distribution over c, a and d sites, the valence and magnetic states of ions, and the incompleteness of the anionic sublattice are in full agreement both with the results of thermodynamic analysis and with experimental investigations of the crystal and magnetic structures of the garnets $\text{R}_{3-x}\text{Bi}_x\text{Sc}_y\text{Fe}_{5-y-z}\text{Ga}_z\text{O}_{12-8}$.

The comprehensive analysis of the garnet structure made it possible to predict the $\mu_{\text{eff}}(c)$ value without magnetic measurements and to determine the compositions with the optimum characteristics, which is indicated by the maxima on the $\mu_{\text{eff}}(z)$ curve, equal to $\sim 16 \mu_{\text{B}}$ ($z = 2$, $x = 1$) and larger than $11 \mu_{\text{B}}$ ($z = 1.8$, $x = 1.5$), observed for the first time for $\text{Dy}_{3-x}\text{Bi}_x\text{Sc}_{0.75}\text{Ga}_z\text{Fe}_{4.25-z}\text{O}_{12}$ that we synthesized. New promising magneto optically active garnets were predicted and the reasons for the appearance of maxima on the $\mu_{\text{eff}}(z)$ plot were explained theoretically; the occurrence of these maxima implies that magnetic properties can be improved even when a ferromagnetic matrix has been diluted by diamagnetic ions.

The comprehensive study of the garnet structure, the formulated postulates, and thermodynamic analysis of garnet formation can be extended to other crystals containing coordinatively nonequivalent positions of atoms, occupied by heterovalent ions in HS or LS states.

References

1. A. M. Balbashov, F. V. Lisovskii, and V. K. Raev, *Elementy i ustroystva na tsilindricheskikh magnitnykh domenakh. Spravochnik* [Elements and Devices on Cylindrical Magnetic Domains. Handbook], Eds. N. N. Evikhieva and B. N. Naumova, Radio i svyaz', Moscow, 1987, 488 pp. (in Russian).
2. J. Haïma, J. A. Pistorius, and D. Mateika, *J. Cryst. Growth.*, 1990, **102**, 974.
3. D. Mateika, E. Volkel, and J. Haïma, *J. Cryst. Growth.*, 1990, **102**, 994.
4. J. Haïma, L. C. Daamas, F. A. De Jong, B. H. Koek, J. W. E. Maes, D. Mateika, J. A. Pistorius, and P. J. Roksnoer, *J. Cryst. Growth.*, 1990, **102**, 1014.
5. R. D. Shannon and C. T. Prewitt, *Acta Crystallogr.*, 1969, **25**, 925.
6. Yu. P. Vorob'ev, *Kristallografiya*, 1989, **34**, 1461 [*Sov. Phys.-Crystallogr.*, 1989, **34** (Engl. Transl.)].
7. V. G. Bamburov, A. S. Vinogradova-Zhabrova, and N. I. Lobachevskaya, *Khimiya tverdogo tela* [Solid-State Chemistry], UrO RAN, Ekaterinburg, 1997, 90 (in Russian).
8. I. S. Kulikov, *Termodinamika oksidov. Spravochnik* [Oxide Thermodynamics. A Handbook], Metallurgiya, Moscow, 1986, 344 (in Russian).
9. S. Krupichka, *Fizika ferritov i rodstvennykh im magnitnykh oksidov* [Physics of Ferrites and Related Magnetic Oxides], 1, Mir, Moscow, 1976, 353 (Russ. Transl.).
10. V. S. Sidorov, E. N. Korobeinikov, S. A. Potylitsyna, and S. K. Timoshenko, *Neorg. Materialy* [Inorg. Mater.], 1997, **33**, 752 (in Russian).
11. Yu. P. Vorob'ev and O. V. Karban', in *Khimiya tverdogo tela i novye materialy* [Solid-State Chemistry and New Materials], UrO RAN, Ekaterinburg, 1996, **2**, 22 (in Russian).
12. F. Bertaux and F. Forrat, *Compt. Rend.*, 1956, **242**, 382.
13. T. Okuda, N. Koshizuka, K. Hayashi, T. Takahashi, H. Kotani, and H. Yamamoto, *IEEE Trans. J. Magnetism in Japan*, 1988, **3**, 483.
14. H. Takouchi, K. Shinagawa, and S. Taniguchi, *Japan J. Appl. Phys.*, 1973, **12**, 465.
15. O. Yu. Goncharov, Yu. P. Vorob'ev, and O. V. Carban, *J. Phys. IV France*, 1997, **7**, No. 3, C1-185.
16. T. Okuda, N. Koshizuka, K. Hayashi, T. Takahashi, H. Kotani, and H. Yamamoto, *J. Magn. Soc. Jpn.*, 1987, **11**, No. 1, 179.
17. T. Okuda, T. Katayama, K. Saton, T. Oikawa, H. Yamamoto, and N. Koshizuka, *Proceed. Fifth Symp. on Magnetism and Magnetic Materials*, Taipei, Taiwan, April 1989, World Scientific, 61.
18. T. Okuda, T. Katayama, K. Saton, and H. Yamamoto, *J. Appl. Phys.*, 1991, **69**, No. 8, IIA, 4580.
19. H. Toraya and T. Okuda, *J. Phys. Chem. Solids*, 1995, **56**, 1317.
20. Y. Hosoe, K. Takanashi, H. Yasuoka, R. Suzuki, Y. Sugita, and S. Chikazumi, *J. Phys. Soc. Jpn.*, 1986, **55**, 731.
21. T. Okuda, T. Katayama, H. Kobayashi, and N. Kobayashi, *J. Appl. Phys.*, 1990, **67**, 4944.
22. B. Stroocka, P. Holst, and W. Tolksdorf, *Philips J. Res.*, 1978, **33**, No. 3/4, 186.
23. Yu. D. Tret'yakov, *Khimiya nestekhiometricheskikh oksidov* [Chemistry of Nonstoichiometric Oxides], MGU, Moscow, 1974, 364 (in Russian).
24. A. Thavendrarajah, M. Paradavi-Horvath, and P. E. Wigen, *IEEE Trans. Magn.*, 1989, **25**, 4015.
25. P. Papakonstantinou, B. Teggart, and R. Atkinson, *J. Phys. IV France*, 1997, **7**, C1-475.
26. K. P. Belov, *Usp. Fiz. Nauk*, 1996, **168**, 669 [*Sov. Phys.*, 1996, **168** (Engl. Transl.)].
27. J. van Elp, J. L. Wieland, H. Eskes, P. Kuiper, G. A. Sawatzky, F. M. F. De Groot, and T. S. Turner, *Phys. Rev.*, 1991, **B44**, 6090.
28. K. Hirakawa, H. Kadowaki, and K. Ubikoshi, *J. Phys. Soc. Jpn.*, 1985, **54**, 3526.
29. X. Oudet, *The Rare Earth in Modern Science and Technology*, Plenum Press, New York—London, 1978, 453.
30. V. P. Pashchenko, G. A. Potapov, E. G. Darovskikh, V. S. Abramov, and A. V. Kopaev, *Metallofizika i noveishie tekhnologii* [Metal Physics and the Modern Technologies], 1996, **18**, 47 (in Russian).
31. V. P. Pashchenko, V. S. Abramov, and Z. A. Samoilenko, *Vseros. nauchno-prakt. konf. "Oksidy. Fiziko-khimicheskie svoystva i tekhnologiya"* [All-Russian Scientific and Practical Conference "Oxides. Physicochemical Properties and Technology. Abstrs.], UrGEU, Ekaterinburg, 1998, 143 (in Russian).